

INVESTIGATION OF K-PG BOUNDARY SAND BODIES AT MOSCOW LANDING
ALABAMA, VIA U-PB GEOCHRONOLOGY: IMPLICATIONS FOR END-
CRETACEOUS PALEODRAINAGE AND THE CHICXULUB IMPACT

by

RYAN PATRICK CULP

MATTHEW WIELICKI, COMMITTEE CHAIR
THOMAS TOBIN
MICHELLE WIELICKI
CHARLES SAVRDA

A THESIS

Submitted in partial fulfillment of the requirements
for the degree of Master of Science
in the Department of Geological Sciences
in the Graduate School of
The University of Alabama

TUSCALOOSA, ALABAMA

2021

Copyright Ryan Patrick Culp 2021
ALL RIGHTS RESERVE

ABSTRACT

Moscow Landing is a well-known Cretaceous-Paleogene (K-Pg) boundary site located in eastern Sumter County Alabama USA and serves as a natural laboratory to study the end-Cretaceous mass extinction given its proximity to the Chicxulub impact. Unique, discontinuous, sand bodies, commonly known as the Clayton sands, mark the contact between Cretaceous and Paleogene rocks. Megawaves generated by the Chicxulub impact and incised valley filling have been cited as the possible mechanisms behind Clayton sand deposition. To further investigate the source of the sediment in the Clayton sands, a multidisciplinary approach is used that involves microscopy (SEM analysis), geochemistry (trace element and major oxides), and detrital zircon U-Pb geochronology. This work represents the first wherein U-Pb geochronological tools have been applied to a K-Pg site in Alabama. Zircon ages reveal an Appalachian-derived sediment signature, with four grains of ~550 Ma possibly indicating a Chicxulub impact-derived source (i.e. Pan-African in age). Shock features within the zircons were not observed, possibly indicating that the ejecta blanket at Moscow Landing was erased or diluted by the subsequent megawave surge as previous research suggests. In addition, the detrital zircon data presented corroborate previous studies in suggesting that the ancestral Mississippi River system was draining large portions of North America at the end-Cretaceous into the Gulf of Mexico as it does today.

DEDICATION

This work is dedicated to my mother Linda, my father Eric, and my sister Sara. Their love and support have been vital to my success as a person and as a student. Thank you for inspiring me to follow my dreams. Love you guys.

LIST OF ABBREVIATIONS AND SYMBOLS

| | |
|--------------------------------|------------------------------|
| U-Pb | uranium-lead |
| Th | thorium |
| U | uranium |
| Th/U | thorium/uranium |
| Pb | lead |
| Zr | zirconium |
| CaO | calcium oxide |
| SiO ₂ | silica oxide |
| Al ₂ O ₃ | aluminum oxide |
| Fe ₂ O ₃ | iron oxide |
| K ₂ O | potassium oxide |
| K-Pg | Cretaceous-Paleogene |
| Ma | millions of years |
| PBC | Prairie Bluff Chalk |
| XRF | X-Ray fluorescence |
| SEM | scanning electron microscopy |
| PDF | planar deformation features |
| µm | micron |
| MEI | methylene iodide |
| % | percent |

\pm plus or minus

> greater than

< less than

LA-ICPMS laser ablation inductively coupled plasma mass spectrometer

ACKNOWLEDGMENTS

I would like to thank my advisor Dr. Matthew Wielicki for guiding me through the research process and keeping me interested in geology. I would also like to thank Dr. Rebecca Totten for allowing me to accompany her micropaleontology class to Moscow Landing in October 2019 and to collect my samples. A special thanks is owed to Dr. Matthijs van Soest and the rest of the team at Group 18 Labs at Arizona State for processing my samples and taking the time to walk me through each step and to control their LA-ICPMS. I want to thank Tyler Wood for allowing me to talk his head off about Moscow Landing and to talk about our complimenting research. I want to thank my lab mates Sam Walker and Jordan Faltys for showing me various lab techniques necessary to the success of this project. I want to also thank them for being two great friends that made my graduate school experience and life better. Dr. Jade Star Lackey and his XRF lab team at Pomona College were a big help with XRF sample analysis and preparation. I would also like to thank my committee members Dr. Tom Tobin, Dr. Michelle Wielicki, and Dr. Charles Savrda for their input and guidance improving this project. Lastly, I want to thank Autumn Anderson for being there for me through all the stress and anxiety throughout this process. Funding was generously given by the Department of Geological Sciences, The University of Alabama Graduate School, and by The University of Alabama CARSCA research grant program.

CONTENTS

| | |
|---|-----|
| ABSTRACT..... | ii |
| DEDICATION | iii |
| LIST OF ABBREVIATIONS AND SYMBOLS | iv |
| ACKNOWLEDGMENTS | vi |
| LIST OF TABLES..... | ix |
| LIST OF FIGURES | x |
| INTRODUCTION | 1 |
| GEOLOGIC BACKGROUND..... | 3 |
| Moscow Landing | 3 |
| Chicxulub Impact Structure and Target Rocks | 4 |
| METHODS | 8 |
| Sample collection and zircon separation..... | 8 |
| Scanning electron microscopy and EDS | 9 |
| X-Ray Fluorescence..... | 9 |
| U-Pb Geochronology | 11 |
| RESULTS | 13 |
| Scanning Electron Microscopy | 13 |
| XRF..... | 13 |
| U-Pb | 17 |
| Sample ML-19-1 | 17 |

| | |
|-------------------------------|----|
| Sample ML-19-2 | 17 |
| Sample ML-19-5 | 18 |
| DISCUSSION | 21 |
| Clayton sand bodies | 21 |
| Prairie Bluff Chalk | 23 |
| XRF | 23 |
| Provenance | 23 |
| Carolina terrane source | 24 |
| Illinois basin source | 25 |
| Yucatan source | 26 |
| CONCLUSIONS | 27 |
| REFERENCES | 29 |

LIST OF TABLES

| | | |
|----|---|----|
| 1. | Whole rock and trace element data..... | 15 |
| 2. | Summarized ~550 Ma U-Pb and Th/U data | 22 |

LIST OF FIGURES

| | | |
|-----|---|----|
| 1. | Paleogeographic map of end-Cretaceous Gulf coast and southern US with sources | 5 |
| 2. | Generalized geologic map of Moscow Landing | 6 |
| 3. | Generalized stratigraphic column of Moscow Landing..... | 7 |
| 4. | Field photo of sandy body 7, samples ML-19-1 and ML-19-2..... | 8 |
| 5. | SEM photos of zircons found at Moscow Landing | 10 |
| 6. | Clastic rock discrimination diagram | 14 |
| 7. | Map of major North American igneous provinces | 16 |
| 8. | Zircon age distribution plot-sample ML-19-2 | 18 |
| 9. | Zircon age distribution plot of sample ML-19-1 and ML-19-5 | 19 |
| 10. | Zircon age distribution from 0 to 1010 Ma for ML-19-1 and ML-19-5 | 20 |
| 11. | SEM images of four ~550 Ma grains with LA-ICPMS spots..... | 22 |

INTRODUCTION

Determining the direct influence of large meteorite impacts on the biosphere requires accurately identifying the impact events within the geologic record and investigating the environmental and biologic response to such high-energy events. One natural laboratory to investigate this is Moscow Landing, a well-documented Cretaceous- Paleogene (K-Pg) boundary location along the west bank of the Tombigbee River in western Alabama (Figures 1 and 2) (Mancini et al., 1989; Savrda, 1993; Pitakpaivan et al., 1994; Savrda, 2018). The sedimentary units below and above the K-Pg boundary at Moscow Landing are the Upper Cretaceous Prairie Bluff Chalk (PBC), and the Lower Paleogene Clayton Formation (Mancini et al., 1989; Savrda, 1993). The disconformity between these two units (Mancini et al. 1989; Savrda, 2018) is locally marked by thin (2-4 m), discontinuous sand bodies informally known as Clayton sands. The primary purpose of this study is to investigate if there is evidence (i.e., shocked zircon, detrital zircon U-Pb ages associated with the Yucatan) at Moscow Landing that can trace the origins of these sand bodies back to the Chicxulub impact. Impact derived zircons relating to Chicxulub have been found at locations around the globe (Krogh et al., 1993a, 1993b; Kamo et al., 2011) and can be used as conclusive evidence that these areas were directly influenced by the impact, highlighting the worldwide influence of such events. Samples were collected at Moscow Landing from both Clayton sands and the Prairie Bluff Chalk. Certain samples were dated via U-Pb geochronology to identify any ages that link back to Chicxulub. Samples were analyzed via XRF for whole-rock and trace-element data to look for any similarity between sand bodies. Scanning electron microscopy (SEM) and electron dispersive spectroscopy (EDS) analysis were

used to image the zircons and to look for impact shock features (PDFs, twin laminae) within the zircon grains as well as to analyze inclusions. This study, the first to apply zircon geochronology to an Alabama K-Pg boundary section, has implications for the Chicxulub impact and end-Cretaceous drainage around the Mississippi embayment.

GEOLOGIC BACKGROUND

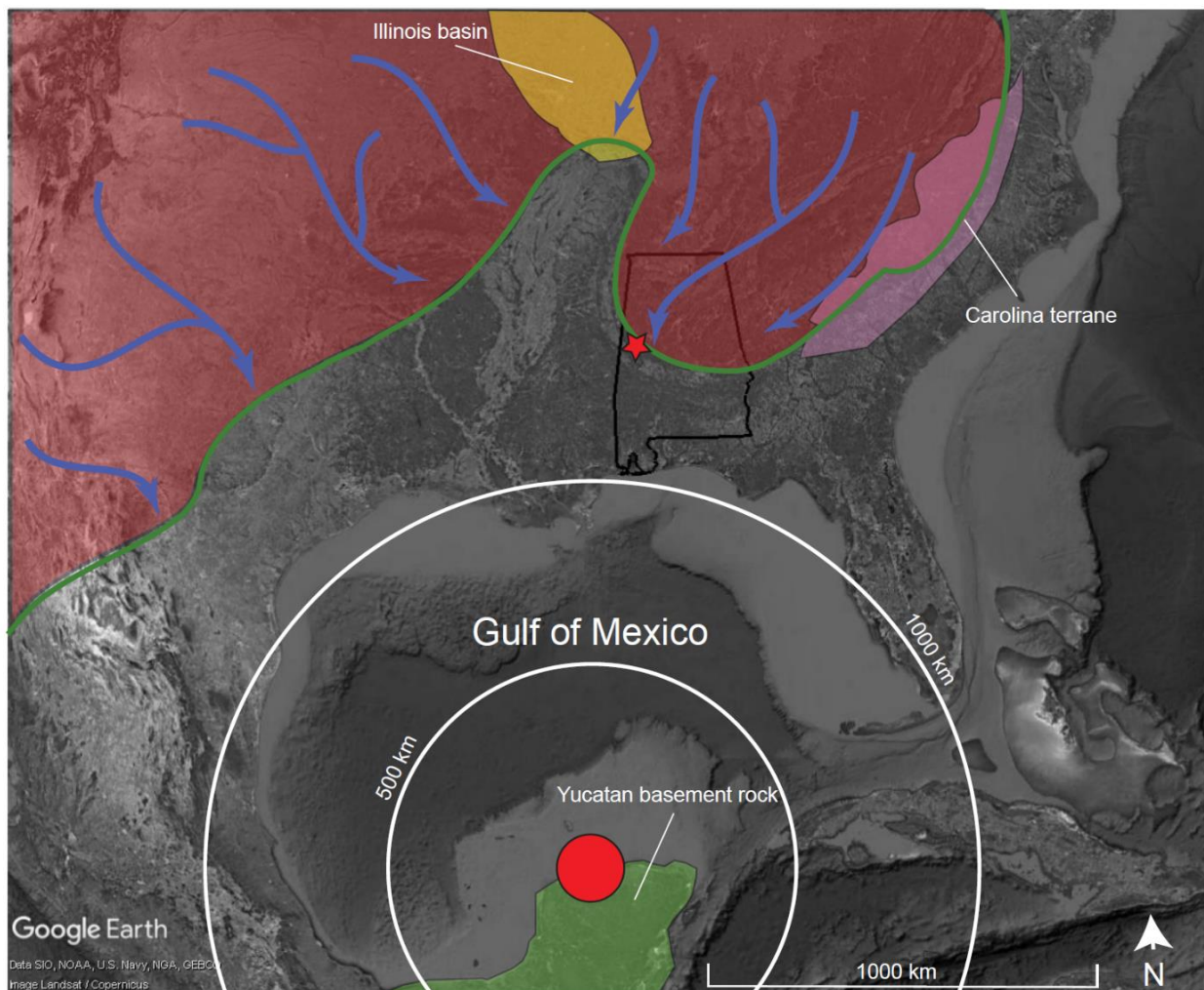
Moscow Landing

Moscow Landing is a natural laboratory to study the relatively local effects of a large-scale bolide impact. This locality lies only ~1200 km from the Chicxulub crater (Figure 1; Hildebrand et al., 1991), and previous work suggests that the section includes impact-related materials, such as altered tektites (Pitakpaivan et al., 1994; Smit et al., 1996; Savrda, 2018). The Moscow Landing section exposes the Cretaceous Prairie Bluff Chalk, which comprises gray, massively bedded, silty to sandy, fossiliferous chalk (Mancini et al., 1989; Savrda, 2018), and the Paleogene Clayton Formation, which comprises deep, undifferentiated shelf facies (Savrda, 2018; Figure 2). At least seven discontinuous sand bodies are emplaced at the contact between the Prairie Bluff Chalk and the Clayton Formation proper (Figure 3). These sand bodies are known as Clayton sands (Mancini et al., 1989; Savrda, 1993; Savrda, 2018). The positions of several of these appear to have been controlled by normal faulting thought to be induced by the impact (Smit et al., 1996; Hart et al., 2016; Savrda, 2018). Previous works have suggested that the Clayton sands formed as incised valley fills associated with sea-level fall and subsequent transgression (Mancini et al., 1989; Savrda, 1993). However, more recently, the Clayton sands have been interpreted to have been emplaced by megawaves generated by the Chicxulub impact (Smit et al., 1994; Smit et al., 1996; Savrda, 2018). Moreover, impact-related spheroids, interpreted as altered tektites (Pitakpaivan et al., 1994), have been found in some Clayton sand bodies at Moscow Landing (Smit et al., 1996) and elsewhere in western Alabama, providing additional evidence that the K-Pg boundary at Moscow Landing contains impact signatures.

Chicxulub Impact Structure and Target Rocks

The Chicxulub impact structure is 180-300 km in diameter (Hildebrand et al., 1991; Sharpton et al., 1993) and sits off the present-day Yucatan Peninsula (Kring et al., 2017). Distal K-Pg ejecta deposits are found globally, many containing high concentrations of iridium first identified by Alvarez et al. (1980) as being extraterrestrial in origin. The age of the Yucatan target rock has been reported as 550 ± 10 Ma based on previous U-Pb dating (Krogh et al., 1993; Kamo and Krogh, 1995; Kamo et al., 2011; Ross et al., 2019). However, Krogh et al. (1993) reported some impact breccia zircon ages of 418 ± 4 Ma from Haiti. These values are crucial in correlating K-Pg sites back to the impact target rocks.

Recently, IODP-ICDP expeditions have reported on the events directly following the impact (Gulick et al., 2019). Data suggest that a tsunami was generated upon impact and reached the far side of the proto-Gulf of Mexico within 2-3 hours after the impact (Gulick et al., 2019). This is consistent with the findings of Smit et al. (1994) and Savrda (2018) that indicate that the Clayton sand bodies at Moscow Landing may have been emplaced by megawaves. It also may explain why there seems to be a lack of impact signatures at Moscow Landing; the megawave could have erased any previously deposited ejecta blanket as the ejecta arrives prior to the initial megawave surge (Lawton et al., 2004).



1

Figure 1. Map showing the generalized US end-Cretaceous coastline. Red star denotes the location of Moscow Landing. The colored polygons denote the three potential sources of 4 ~550 Ma zircons (refer to the discussion). Sources given in the map legend.

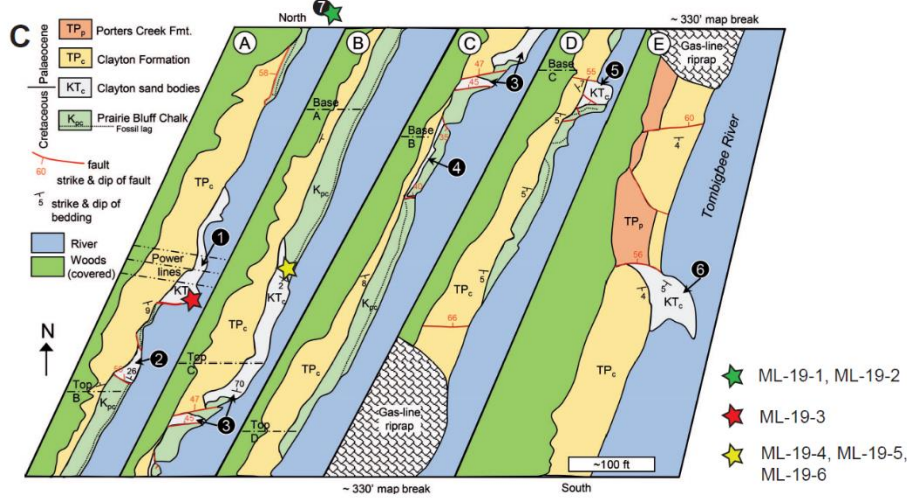
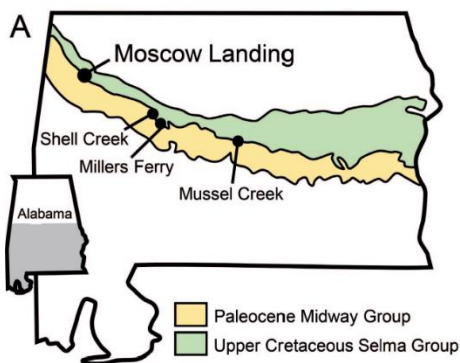


Figure 2. (A) Map of the upper Cretaceous and lower Paleogene rocks across central Alabama. (B) Satellite map of Moscow Landing along the west bank of the Tombigbee River, the white arrow indicates where Clayton sand body 7 is located. Boxes A-E correspond to the strip maps in part C of this figure. (C) Generalized geologic map of the Moscow Landing section exposed. This study addressed sand body 7 which is off map just to the north of A (all portions of this figure modified from Savrda, 2018).

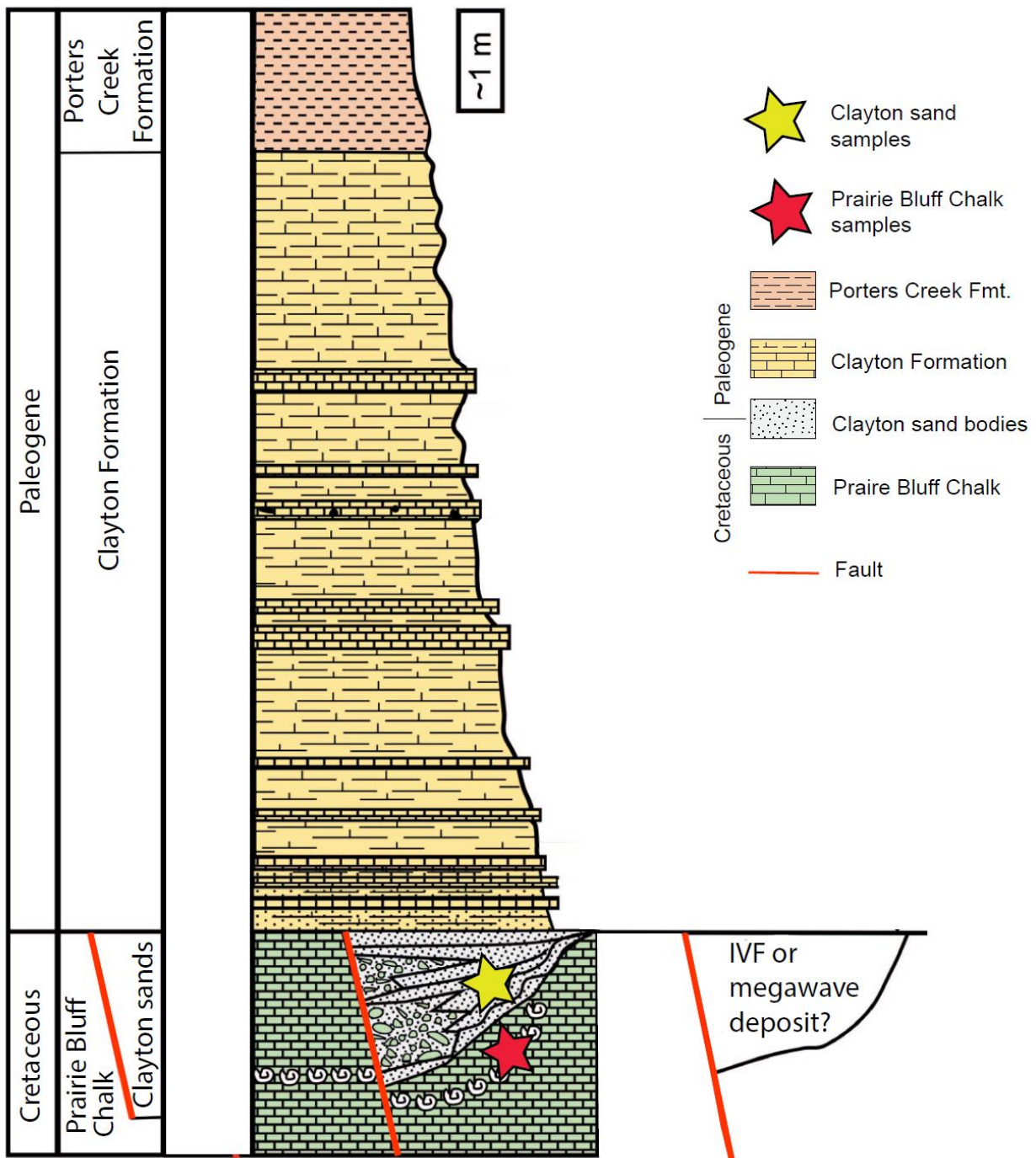


Figure 3. Stratigraphic column of the rocks exposed at Moscow Landing. The Cretaceous Prairie Bluff Chalk in green and the Paleogene Clayton formation in yellow. The Clayton sands occur at the contact between those two units (modified from Savrda, 2018).

METHODS

Sample Collection and Zircon Separation

Six samples were collected from three localities along the Tombigbee River near Moscow Landing, eastern Sumter County, Alabama in October of 2019. A stratigraphic column (Figure 3) and map (Figure 2C) by Savrda (2018) were used to determine sample locations. Samples weighing 1-2 kg were collected directly above and below the K-Pg boundary, from the Clayton sands and the PBC, respectively (Figure 4). Four Clayton samples were collected from sand bodies 1, 3, and 7 and two PBC samples were collected from directly below sand bodies 3 and 7 (Figure 2).

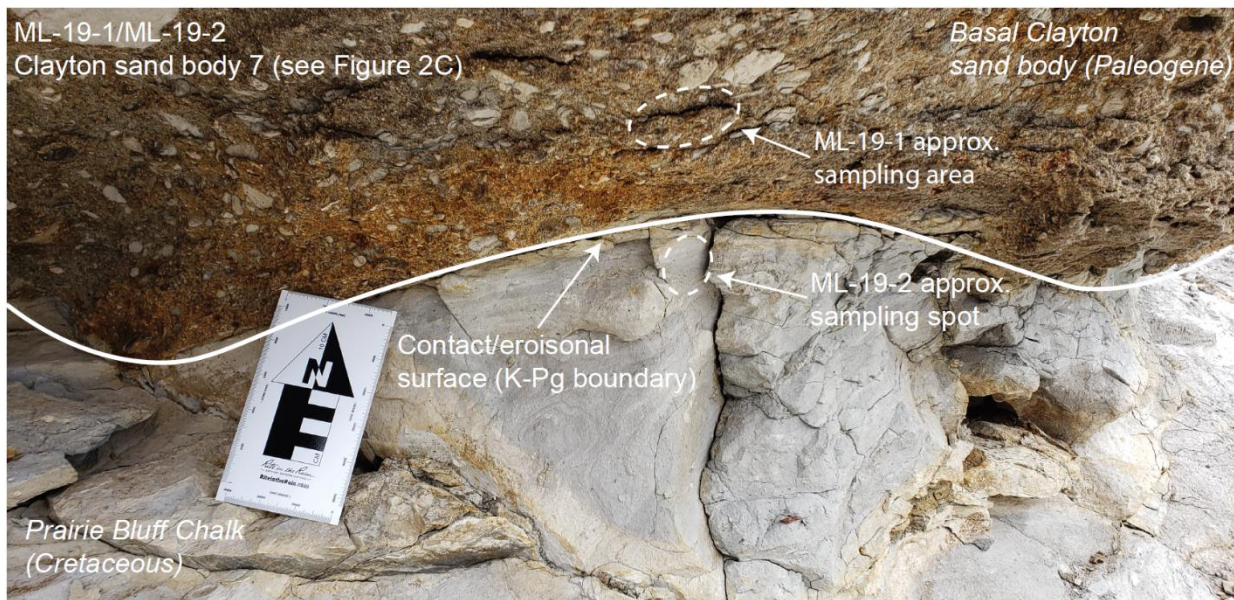


Figure 4. Field photo from Moscow Landing. Photo showing the contact between the Prairie Bluff Chalk and one of the seven Clayton sand bodies exposed at Moscow Landing.

Samples were processed into individual grains using a jaw crusher and disc mill and then put through a 250- μ m sieve to isolate single mineral grains (as opposed to aggregates). Decanting with water removed any clay minerals in preparation for heavy liquid separation. Methylene iodide (MEI), which has a specific density of 3.85 g/cm³, was used to isolate zircon from minerals with lower specific gravities (e.g., quartz and feldspar in the Clayton samples, calcareous material in the PBC samples). The sink containing the isolated zircons was collected, rinsed with acetone to remove any excess MEI, and dried under a fume hood. Zircons were then handpicked and mounted into 1-inch epoxy pucks and polished to sub-micron grit.

Scanning Electron Microscopy and EDS

Mounted zircons (Figure 5) were analyzed on a JEOL 7000 FE SEM with an Oxford X-Max 80mm² silicon drift detector, at the Alabama Analytical Research Center (AARC), to look for impact shock features and to determine the compositions of inclusions. A working distance of 10-12 mm and a 20 kV accelerating voltage was used to image each grain. A 15-second point live time was used for each Energy Dispersive Spectroscopy (EDS) analysis.

X-ray Fluorescence

Major oxides and selected trace elements were determined for four Clayton sand and two PBC samples by X-ray fluorescence (XRF) at Pomona College. Samples were prepared using the double fusion technique with a 2:1 ratio adapted from Johnson et al. (1999). The six samples were powdered using a puck and mill. 3.5 g of powdered sample was mixed with 7 g of a dilithium tetraborate

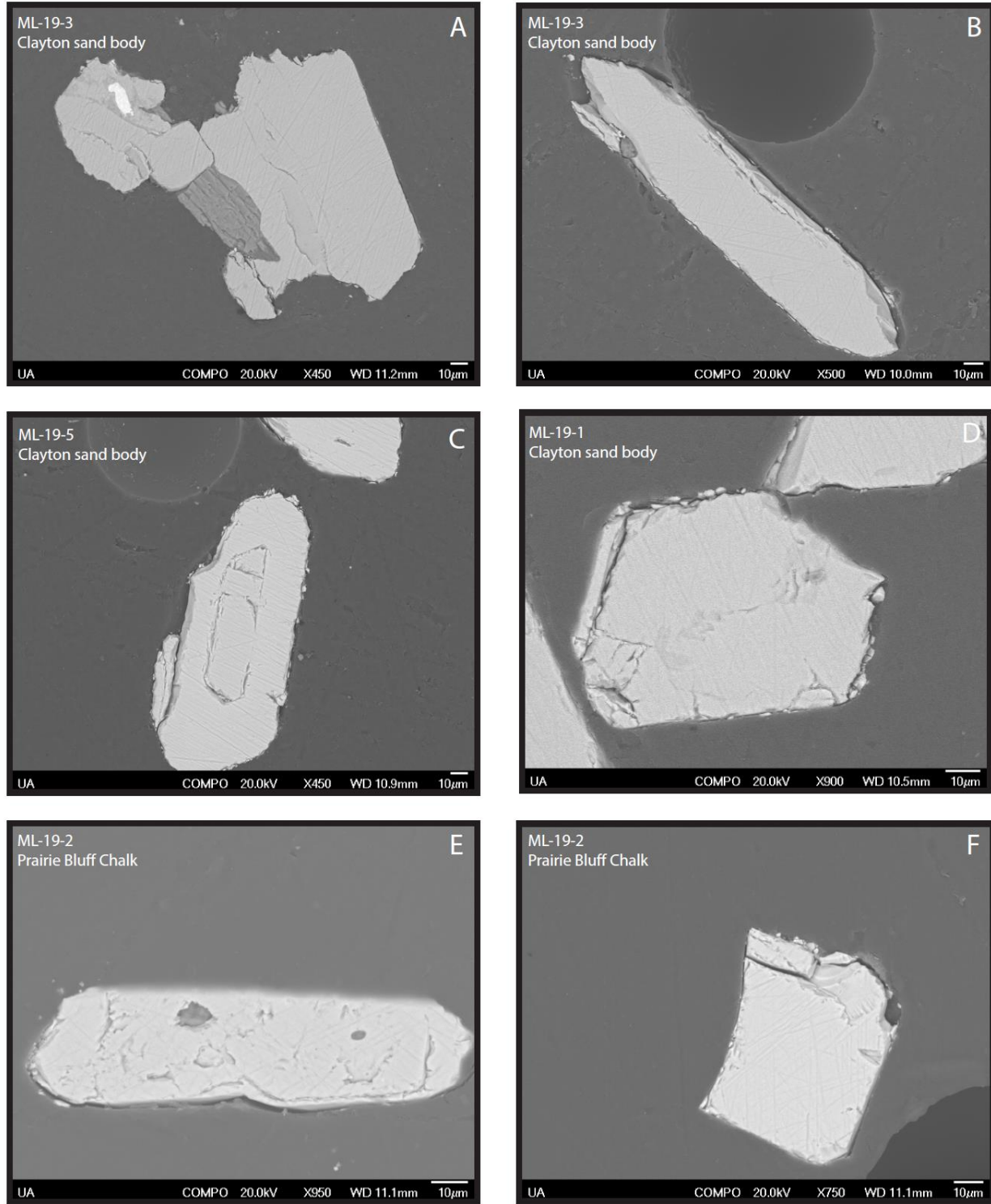


Figure 5. (A-F) SEM images of zircons found in both the Clayton sand bodies and the Prairie Bluff Chalk. SEM analysis shows a variety of shapes and sizes. Zircons found in the Prairie Bluff Chalk are much smaller than the zircons found in the Clayton sand bodies.

flux in a 2:1 ratio. The blended mixture was fused into a glass bead using a graphite crucible at 1000 °C for 5 min, repowered, fused a second time, polished, and analyzed on a 3.0 kW Panalytical Axios wavelength dispersive XRF spectrometer.

U-Pb Geochronology

Three samples mounted in individual epoxy mounts with several co-mounted AS-3 zircon standards were loaded into the sample tray of the HelEx II Active two volume ablation cell mounted on a Photon Machines (now CETAC/Teledyne) Analyte G2 193nm UV Excimer laser-ablation system, together with a mount containing a variety of age standards. For two Clayton sand samples (ML-19-1 and ML-19-5), a 35- μm spot size was used, while for chalk sample ML-19-2 the small grain size of some of the zircons necessitated the use of a 25- μm spot size. Aside from the different spot size for sample ML19-2, all laser settings during the analysis of the three samples were the same; a base laser energy output of 4 mJ at a repetition rate of 10Hz was employed, and the beam was attenuated to allow 40% of the initial beam energy to reach the sample leading to an estimated fluence at the sample of ~3 J/cm². Helium was used as an ablation cell and carrier gas set at 0.2 and 0.6 l/m respectively, and 10 ml/m of nitrogen was introduced to the sample stream after the ablation cell. This sample stream was mixed with ~1 l/m of argon nebulizer gas before introduction to the ICP-MS, a Thermo iCap Qc quadrupole mass spectrometer. Samples were ablated for 30 seconds, preceded by 20-second gas blank, and followed by a 15-to-20-second washout period and were analyzed using sample-standard bracketing. Aside from the co-mounted AS-3 (1099Ma; Paces & Miller, 1993; Schmitz et al., 2003; Mattinson, 2010) zircon standard, zircon U-Pb standards FC-1 (1099Ma; Paces & Miller, 1993; Schmitz et al., 2003; Mattinson, 2010), Plesovice (337Ma; Slama et al., 2008), and 94-35 (55.5Ma; Klepeis et al., 1998) were used during the analytical runs. FC-1 was used as the

primary standard for both down-hole fractionation corrections and age normalizations, while the others served as check standards (Horstwood et al., 2003; Paton et al., 2011; Ver Hoeve et al., 2018). The following isotopes were analyzed with their respective dwell times given in parentheses: ^{202}Hg (20ms), ^{204}Pb (50ms), ^{206}Pb (80ms), ^{207}Pb (100ms), ^{208}Pb (10ms), ^{232}Th (10ms), ^{238}U (40ms). ^{235}U was not analyzed because on the instrument count yields are generally so low that estimating ^{235}U from ^{238}U using the natural $^{238}\text{U}/^{235}\text{U}$ ratio of 137.818 (Hiess et al., 2012) gives better results. The data were reduced using Iolite 3.71 (Paton et al., 2010), and specifically the VizualAge data reduction scheme (Petrus and Kamber, 2012) that allows for ^{204}Pb -based common-Pb corrections. Common lead corrections were only applied to analyses that had ^{204}Pb counts significantly above baseline, which was only necessary in a small number of analyses. $^{206}\text{Pb}/^{238}\text{U}$, $^{207}\text{Pb}/^{235}\text{U}$, and $^{207}\text{Pb}/^{206}\text{Pb}$ ratios were exported from Iolite, and IsoplotR (Vermeesch, 2018) was used to calculate the ages reported. All detrital zircon probability density plots (PDP) were made using Density Plotter with a bin size ranging from 60 – 78 Ma with no smoothing applied (Vermeesch, 2012). All raw data can be found in the supplementary appendix.

RESULTS

Scanning Electron Microscopy

SEM analysis shows a variety of morphologies from round anhedral to euhedral zircons in a variety of sizes ranging from 60 microns (sample ML-19-2) to 200 microns (ML-19-1, ML-19-5). EDS analysis of zircons reveals a variety of inclusions including quartz, feldspar, titanite, and thorite. Quartz and feldspar were the dominant inclusions followed by titanite with one grain containing thorite (Figure 5A). PDFs and shock features were not observed in any of the zircons analyzed but should not be ruled out as being present at Moscow Landing as four of the seven Clayton sands were not collected/analyzed.

XRF

Trace elements and major oxides for samples collected at Moscow Landing are summarized in Table 1. The Clayton sand samples show a range of SiO₂ (59.59-76.67wt.%), Al₂O₃ (1.78-4.81wt.%), Fe₂O₃ (3.77-14.51wt.%), K₂O (0.56-0.84wt.%), and CaO (14.94-23.33 wt.%). The Prairie Bluff samples show a narrower range of SiO₂ (18.21-25.81 wt.%), Al₂O₃ (3.22-7.74 wt.%), Fe₂O₃ (4.24-5.93 wt.%), K₂O (0.56-1.34 wt.%) and CaO (56.50-71.84 wt.%). All four Clayton sand samples plot in the Fe-sand area in a sandstone discrimination diagram (Herron, 1988; Figure 6). Sample ML-19-4 was taken at the contact between the PBC and sand body 3 (Figure 4), which is why it seems to show a higher iron-oxide percentage compared to the other samples.

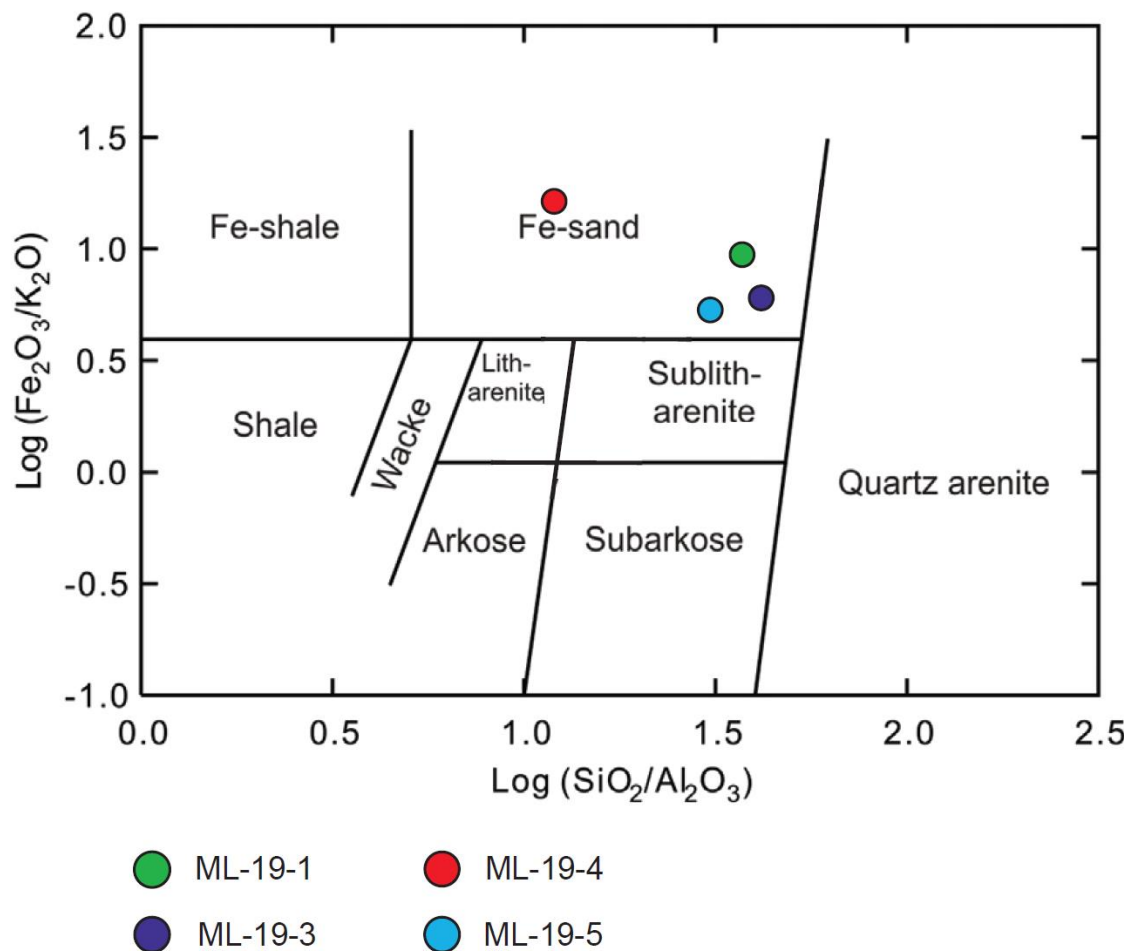


Figure 6. Clastic sedimentary rock discrimination diagram comparing the whole-rock chemistry of each Clayton sand body sample to each other. Samples ML-19-4 and ML-19-5 were taken from sand body 3. ML-19-4 is from the contact between the Prairie Bluff Chalk and the Clayton sand body, and ML-19-5 was taken from the top of the Clayton sand body (scheme from Herron, 1988 and modified from Chen et al., 2020).

Table 1.

Whole-rock and trace element analysis of the Prairie Bluff Chalk and Basal Clayton Sands at Moscow Landing, Alabama

| Sample | ML-19-1 Clayton Sand | ML-19-2 Prairie Bluff Chalk | ML-19-3 Clayton Sand | ML-19-4 Clayton Sand | ML-19-5 Clayton Sand | ML-19-6 Prairie Bluff Chalk |
|--------------------------------|----------------------|-----------------------------|----------------------|----------------------|----------------------|-----------------------------|
| wt. % | | | | | | |
| SiO ₂ | 70.54 | 25.81 | 76.67 | 59.59 | 68.44 | 18.21 |
| TiO ₂ | 0.08 | 0.45 | 0.07 | 0.27 | 0.10 | 0.20 |
| Al ₂ O ₃ | 1.78 | 7.74 | 1.65 | 4.81 | 2.31 | 3.22 |
| Fe ₂ O ₃ | 5.04 | 5.93 | 4.50 | 14.51 | 3.77 | 4.24 |
| MnO | 0.05 | 0.08 | 0.06 | 0.02 | 0.08 | 0.11 |
| MgO | 0.26 | 1.06 | 0.23 | 0.62 | 0.34 | 0.60 |
| CaO | 18.67 | 56.50 | 14.94 | 15.48 | 23.33 | 71.84 |
| Na ₂ O | 0.07 | 0.15 | 0.11 | 0.16 | 0.23 | 0.12 |
| K ₂ O | 0.63 | 1.34 | 0.60 | 0.84 | 0.64 | 0.56 |
| P ₂ O ₅ | 2.75 | 0.64 | 1.08 | 3.53 | 0.67 | 0.60 |
| Total | 99.88 | 99.72 | 99.91 | 99.82 | 99.88 | 99.70 |
| ppm | | | | | | |
| Rb | 19 | 64 | 16 | 29 | 20 | 34 |
| Sr | 406 | 1268 | 259 | 636 | 407 | 1730 |
| Ba | 145 | 203 | 124 | 214 | 135 | 140 |
| Zr | 45 | 159 | 53 | 77 | 56 | 73 |
| Y | 23 | 19 | 18 | 29 | 14 | 16 |
| Nb | 4 | 11 | 4 | 5 | 3 | 7 |
| Mo | 10 | - | 8 | 22 | - | - |
| Cs | 9 | - | - | - | - | 20 |
| Sc | 12 | 17 | 8 | 14 | 13 | 11 |
| V | 27 | 77 | 21 | 60 | 30 | 44 |
| Cr | 45 | 108 | 47 | 62 | 45 | 68 |
| Ni | 39 | 51 | 34 | 49 | 30 | 34 |
| Cu | 63 | 72 | 60 | 75 | 107 | 85 |
| Zn | 23 | 88 | 11 | 44 | 45 | 56 |
| Ga | 3 | 12 | 3 | 3 | - | 9 |
| La | 18 | 32 | 9 | 37 | 14 | 23 |
| Ce | 41 | 58 | - | 45 | - | 49 |
| Pr | 4 | 12 | 3 | 8 | 4 | 10 |
| Nd | 24 | 28 | - | 28 | - | 39 |
| Hf | - | 14 | - | 8 | - | 12 |
| Ta | - | - | - | - | - | - |
| Pb | 8 | 4 | 9 | 9 | 9 | - |
| Th | 7 | 32 | 7 | 16 | 11 | 42 |
| U | 13 | 6 | 7 | 16 | - | - |

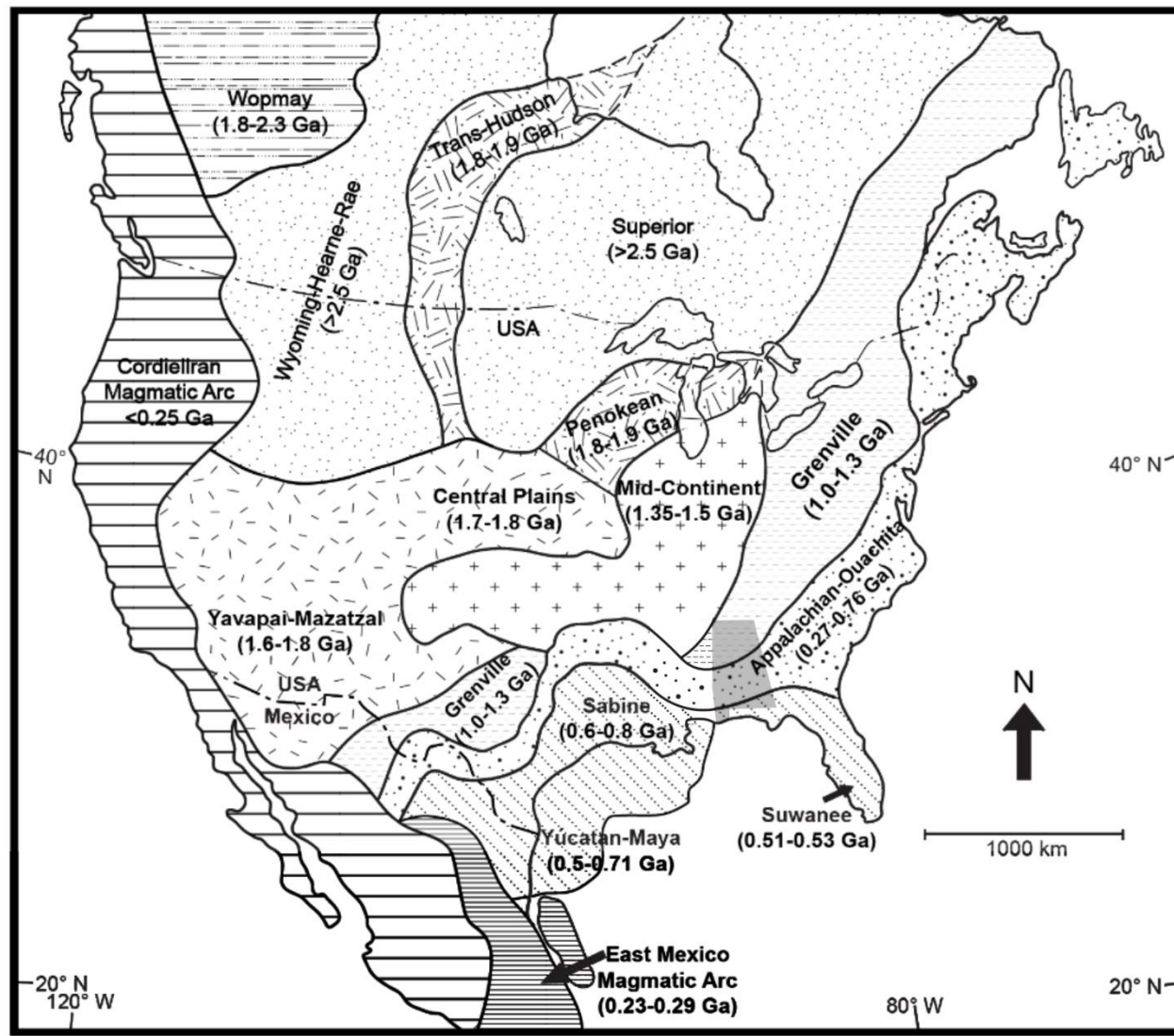


Figure 7. Map of major North American igneous provinces and their ages. Gray polygon is the state of Alabama. Ages correspond to age colors in figures 8, 9, and 10. Modified from Gifford et al. (2020) and sources therein.

U-Pb

Detrital zircons were dated via U-Pb geochronology from the Clayton sand (samples ML-19-1-2 and ML-19-5), as well as from the Prairie Bluff Chalk (sample ML-19-2). The zircons yield ages that correspond to major North American igneous province age ranges published by Gifford et al. (2020; Figure 7), dominated by Grenville, Acadian, and Taconic, with minor components of Pan-African/Gondwanan, Yavapai-Mazatzal, Mid-Continent/Granite-Rhyolite, Trans-Hudson, and Superior (Figures 8, 9, and 10). Age results can be found in the supplementary appendix.

Sample ML-19-2

Twenty-four (24) zircons were dated in sample ML-19-2 with ages ranging from 382.7 ± 4.5 Ma to 1088 ± 10 Ma (Figure 8). Only 24 zircons were isolated, as chalk is not a lithology that normally contains large amounts of siliciclastic minerals. Grenville is the dominant age (~33%) followed by Acadian (~21%), Gondwanan (~13%) and equal percentages of Yavapai-Mazatzal, Taconic, and Alleghenian (~8%).

Sample ML-19-1

One hundred and thirty-one (131) zircons were dated in sample ML-19-1 with ages ranging from 187.2 ± 2.7 Ma to 1389.2 ± 7.8 Ma (Figures 9 and 10). Grenville is the dominant age (~53%) followed by Acadian (~25%), Gondwanan (~8%), Taconic (~7%), and Alleghenian (~2%) age zircons. One zircon recorded an age of 187 Ma which is 109 Ma younger than the next youngest zircon and could represent input from a source farther to the west (Figure 8).

Sample ML-19-5

One hundred and eighty-nine (189) zircons were dated in sample ML-19-5 with ages ranging from 322.1 ± 3.1 Ma to 2657 ± 26 Ma. Grenville is the dominant age (~44%), followed by Acadian (~24%), Taconic (~12%), Gondwanan (~4%), and Alleghanian (~3%) ages (Figures 8 and 9). What is notable about this sample is that there are Mid-Continent Granite-Rhyolite (~6%), Yavapai-Mazatzal (~.5%), Trans-Hudson (~.5%), and Superior (~.5) ages that are not present in the other two samples except for the Yavapai ages in sample ML-19-2. Zircons 007, 058, 121, and 162 recorded ages of 543.7 ± 5.2 Ma, 555 ± 11 Ma, 545 ± 18 Ma, and 544.6 ± 6.8 respectively and are within error of the previously published Yucatan basement age of 550 ± 10 Ma (Krogh et al., 1993a; Krogh et al., 1993b; Table 2; Figure 10).

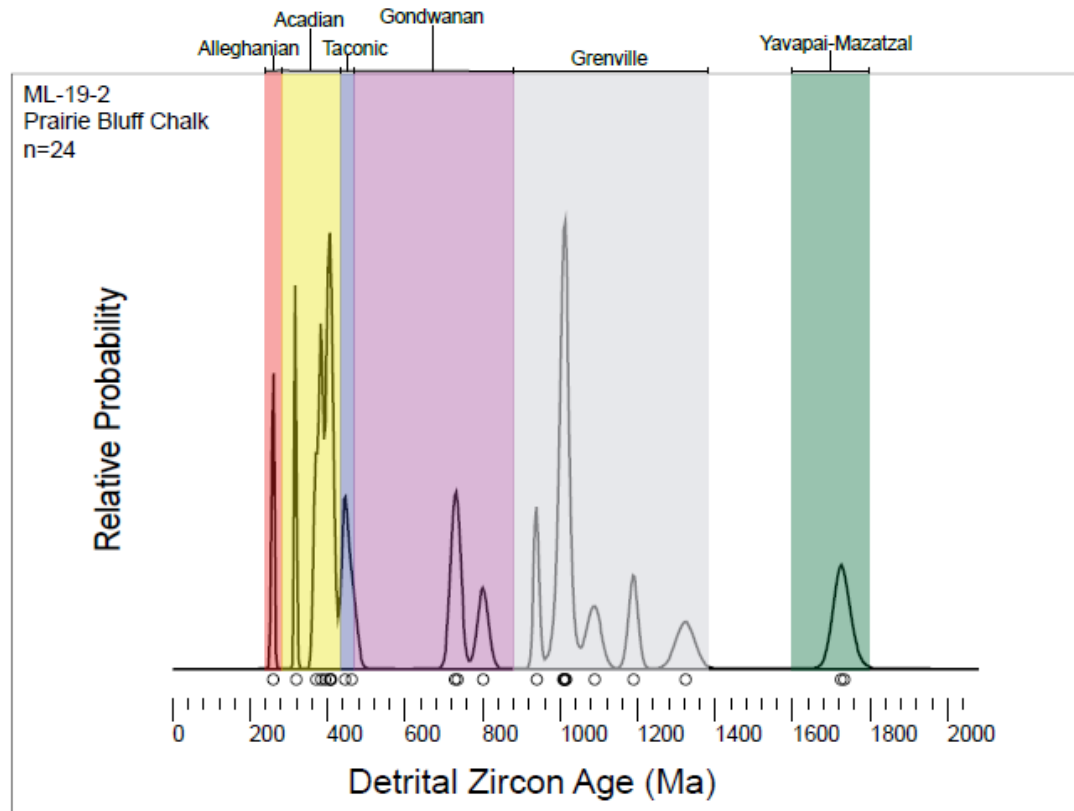


Figure 8. PDP plot showing the zircon ages found in Prairie Bluff Chalk sample ML-19-2. Bimodal signature with one mode of Grenville and the other of Acadian/Taconic.

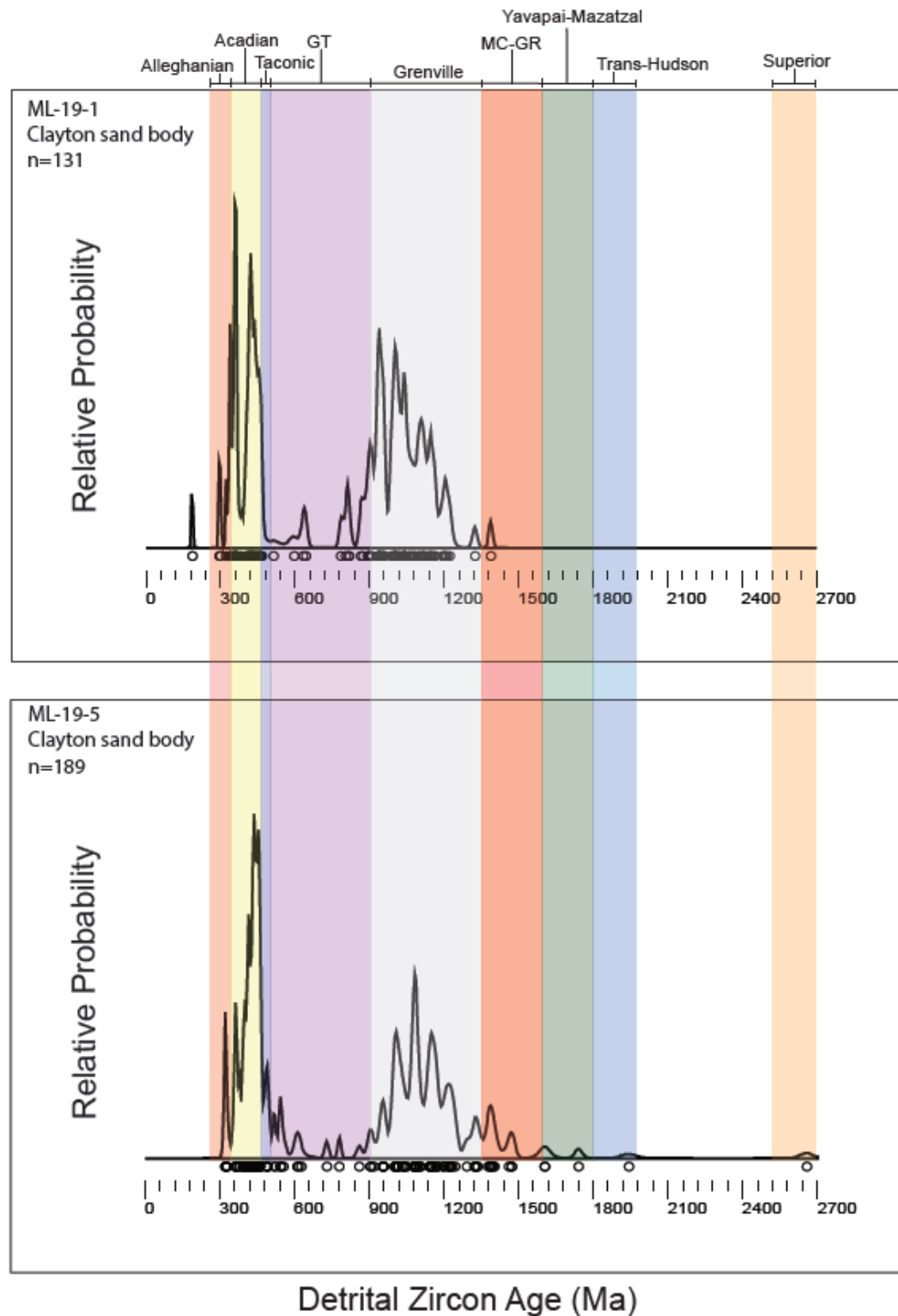


Figure 9. PDP plot showing the zircon ages of the two Clayton sand body samples ML-19-1 and ML-19-5. Both plots show similar age and bimodal distributions. However, sample ML-19-5 has a minor mode around 550 Ma which is absent in ML-19-1.

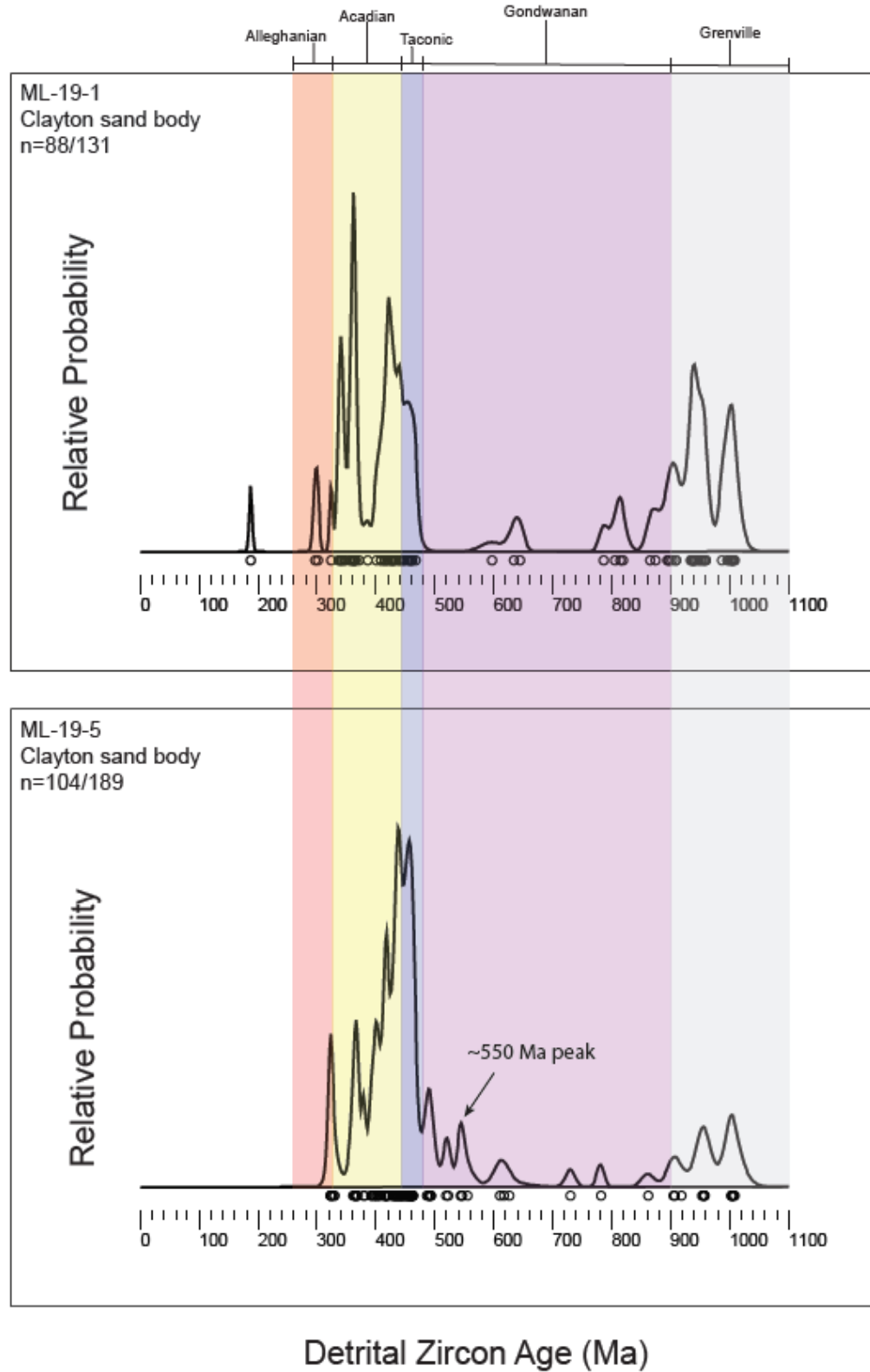


Figure 10. PDP plot showing zircon with ages from 0 to ~1010 Ma for each Clayton sample. Note the ~550 Ma peak in sample ML-19-5 that is not present in ML-19-1.

DISCUSSION

Clayton sand bodies

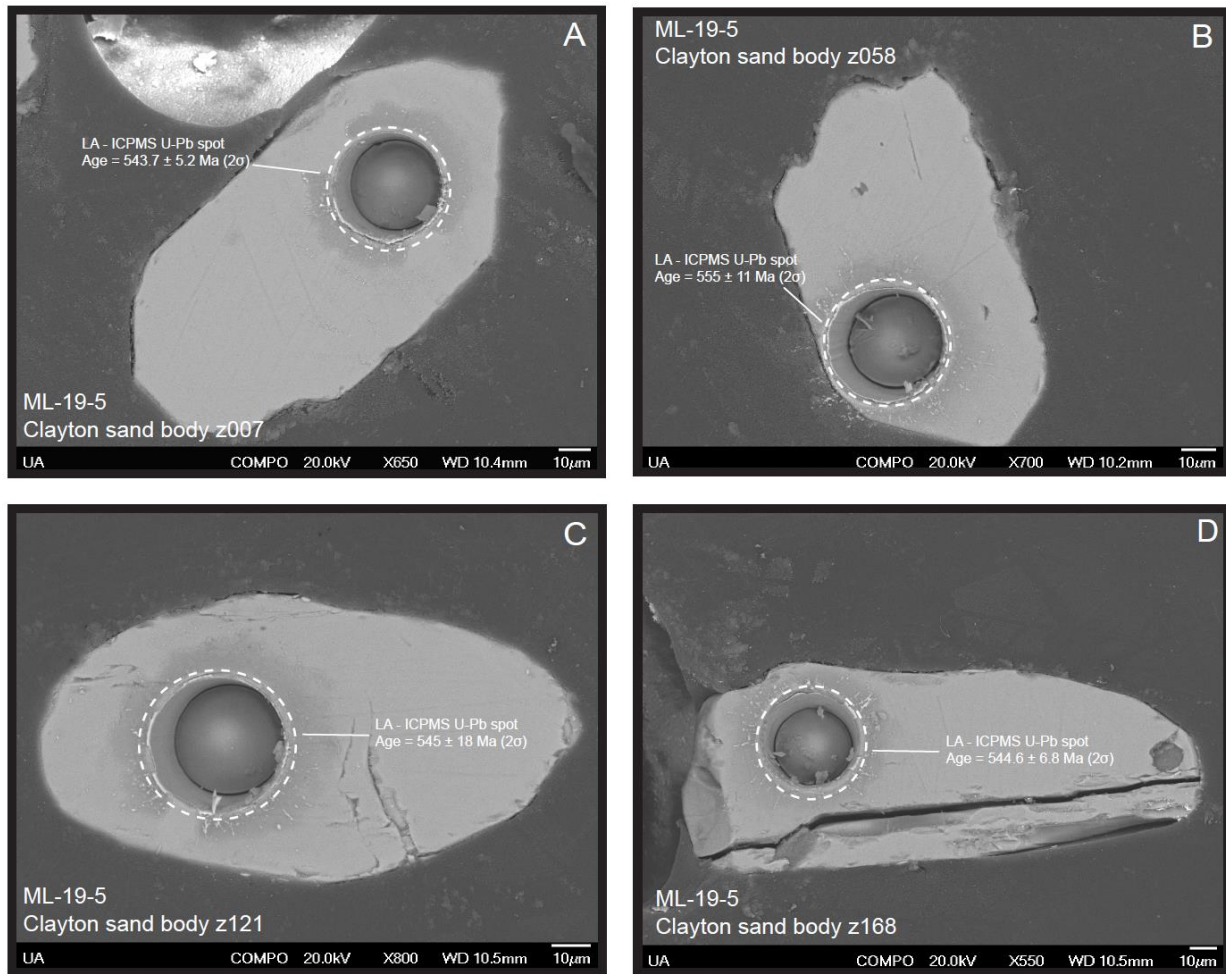
The two different Clayton sand bodies analyzed (ML-19-1 and ML-19-5) for age data are similar to each other and both show a bimodal age distribution (Figures 9 and 10), although ML-19-1 (n=131) lacks the ~550 Ma peak present (n=4; Figure 9) in ML-19-5 (n=189; Figure 11). This could because more zircons were analyzed in ML-19-5. Though the two samples analyzed have very similar age distributions, it cannot be determined if they are representative of all Clayton sand distributions without further analysis.

Shock features were not observed in zircon grains from the Clayton sand bodies. This is probably not due to annealing as it is unlikely that the Clayton sand bodies were ever at a temperature ($T>400$ °C; Zhang et al., 2000) high enough to erase planar features; zircons are resistant to most post-depositional processes. Zircons associated with Chicxulub (both shocked and unshocked) can travel thousands of kilometers from the impact site, either as ejecta or via river drainage of ejecta material (Krogh et al., 1993a; Kamo et al., 1995; Kamo et al., 2011; Cavosie et al., 2020) and were expected to be present in the Clayton sand bodies if they did form shortly after the impact. However, other research has indicated that an ejecta blanket was emplaced around the Gulf coastal plain but was subsequently eroded by the megawave surge (Lawton et al., 2004). This could possibly explain both the lack of shocked minerals and a defined extraterrestrial trace-element layer within the K-Pg deposits at Moscow Landing.

Table 2.

Summarized zircon (U-Pb) plus Th/U data of 4 grains from sample ML-19-5

| Lithology | Sample | Conchordant Age (Ma) | Error (2σ) | % Discordance | Th/U | Error (2σ) |
|-----------------|--------------|----------------------|---------------------|---------------|--------|---------------------|
| Basal Sandstone | ML-19-5 z007 | 543.7 | 5.2 | 1.03 | 0.503 | 0.010 |
| | ML-19-5 z058 | 555 | 11 | 7.76 | 0.1230 | 0.0050 |
| | ML-19-5 z121 | 545 | 18 | -0.35 | 0.145 | 0.010 |
| | ML-19-5 z162 | 544.6 | 6.8 | 7.12 | 0.1250 | 0.0067 |

**Figure 11. (A-D)** SEM images of the four early Pan-African grains of interest. Zircon dates correspond to the information in Table 2 (above).

Prairie Bluff Chalk

The presence of zircon found in the PBC is intriguing, especially given the ages present in the distribution. The chalk sample analyzed has a similar bimodal age distribution to that of the Clayton sand samples that show an Appalachian input. However, the presence of Yavapai age (~1.7 Ga, n=2) grains could indicate input from the western/mid-continent portion of the United States. The continental age signature present (Figure 7) and the high amounts of SiO₂ and Al₂O₃ (Table 1) could indicate that the PBC was formed closer to shoreline than previously thought (Savrda, 1993).

XRF

All the Clayton sand body samples plot in the Fe-sand category of a clastic rock discrimination plot (Figure 6) suggesting that the sand bodies were deposited in similar conditions and experienced similar diagenetic conditions. Plotting in the Fe-sand diagram is an indication the samples contain pyrite and/or glauconite (Herron, 1988).

Provenance

As noted in the results, the majority of the zircons dated in this study can be linked to North American igneous provinces (Figure 7). Although they are not associated with the Chicxulub impact, they are nevertheless important in determining sediment sources especially when coupled with Th/U values. As previous works suggests, the end-Cretaceous and early-Paleogene drainage into the present day southern United States seems to have come from the northeast and mid-continent as it does today (Blum and Pecha, 2014; Potter-McIntyre et al., 2018; Gifford et al., 2020 Jackson et al., 2021; Figure 1). Th/U values can help distinguish between metamorphic and igneous sources and when coupled with zircon ages help narrow down potential sources areas. Previous studies indicate that low Th/U (< 0.1) in zircons are

associated with metamorphic crystallization (Jackson et al., 2021 and sources therein). Recent studies about end-Cretaceous/early-Paleogene Gulf Coast paleodrainage seem to indicate that there was Piedmont (predominately metamorphic) derived sediment draining to the southern Gulf Coast and mixing along the coastline with Appalachian foreland derived (predominantly igneous) basin sediment draining to the northern Gulf Coast (Jackson et al., 2021). Th/U values in this study seem to agree with previous studies suggesting a Piedmont derived sediment source but with inputs from the Appalachian foreland basin and mid-continent areas (Jackson et al., 2021).

Four grains from Moscow Landing have ages (~550 Ma) that are relatively rare in North America (Krogh et al., 1993b; Table 2; Figure 10) and are of particular interest to this study. All four grains also have Th/U values > 0.1 possibly indicating an igneous origin rather than metamorphic. Three possible sources for these early Pan-African grains are discussed below and shown in Figure 1.

Carolina Terrane source

The Carolina terrane is an exotic volcanic island arc located in the hinterland of the Appalachian orogen in the eastern United States (Virginia, North Carolina, South Carolina, and Georgia; Figure 11) and is one of many terranes accreted during the assembly of the super-continent Gondwana (Dennis and Wright, 1997; Ingle et al., 2003). Magmatic activity occurred from about 630 Ma to 540 Ma ending with the eruption of the Morrow Mountain rhyolite at the end of Cambrian (Wortman et al., 1999; Ingle et al., 2003).

With the Carolina terrane being exposed throughout many states in the east and southeast, it may be a possible source for the ~550 Ma zircons found at Moscow Landing. This is supported by evidence that the newly formed ancestral Mississippi river was draining a large

portion of the eastern United States through the Gulf of Mexico at the end Cretaceous (Blum and Pecha, 2014, Potter-McIntyre et al., 2018).

Illinois basin source

The Illinois basin (Figure 1) is an oblong structure flanked by the Cincinnati arch to the east and the Kankakee arch to the west (Thomas et al., 2020). The Cincinnati arch separates the Illinois basin from the eastern portion of the Appalachian basin (Thomas et al., 2020).

Three samples reported in Thomas et al. (2020) from the Illinois basin record age distributions with an “Appalachian signature” (Thomas et al., 2017) and contain early Pan-African ages. Two samples were taken from a sandstone member of the Caseyville Formation and one from the Hardinsburg sandstone. The Caseyville is lower to middle Pennsylvanian in age and the Hardinsburg is upper Mississippian in age (Thomas et al., 2020). The sediment in these rocks is thought to be derived from the Alleghenian orogen and to have traveled through the Appalachian basin to their present locations (Thomas et al., 2020).

Other late Cretaceous sandstones, such as the McNairy sandstone, found at the northern part of the Mississippi embayment have been studied and seem to indicate they were sourced from middle to lower Pennsylvanian strata in the Illinois basin (Potter-McIntyre et al., 2018). The Clayton sands exposed at Moscow Landing show a similar zircon signature to both the rocks discussed in Potter-McIntyre et al. (2018) and the Illinois sandstones discussed in Thomas et al. (2020). The ultimate source for the zircons present in the Clayton sands could be from the Illinois basin but the McNairy sandstone may provide a more proximal sediment source to the Clayton sands as the age distribution is similar between the Illinois basin sands, the McNairy sandstone, and the Clayton sands.

Yucatan source

Finally, the Chicxulub impact crater is a possible source for the ~550 Ma zircons found at Moscow Landing (Figure 1). The crystalline rocks underlying the Yucatan platform are heterogenous in age, ranging from ~550-300 Ma with most of the rock being Pan-African in age (Kettrup and Deutsch, 2003; Schmieder et al., 2017; Ross et al., 2019). Krogh et al. (1993a) reported an upper intercept of ~545 Ma for a component of the Yucatan target rock, and Krogh et al. (1993b) reported an upper intercept of ~550 Ma from zircons found at a K-Pg layer in Colorado. The ~550 Ma grains found in this study show a range of discordance (0-7.7%; Table 2) indicating little to no Pb loss. This would be unexpected if they were delivered via hot ejecta. However, the ~550 Ma grains found by Krogh et al. (1993a, b) also show little Pb loss as they plot on concordia which indicates they are relatively unaltered Yucatan grains. Given that the Clayton sand bodies at Moscow Landing are hypothesized as being Chicxulub megawave deposits (Smit et al., 1996; Savrda, 2018) and that some basal sand bodies purportedly contain altered impact spherules (Pitakpaivan et al., 1994), the Yucatan basement cannot be eliminated as a potential source for the Pan-African zircon ages in this study. However, further geochemical research is needed to fully pinpoint the source of Pan-African grains found at Moscow Landing and potentially at other K-Pg sites in southern North America.

CONCLUSIONS

Constraining the local and global environmental effects associated with large impact events requires the accurate identification of these events preserved within geologic strata, including the K-Pg succession exposed at Moscow Landing in western Alabama. Zircons from the Clayton sands at Moscow Landing show an Appalachian age distribution similar to that of other late Cretaceous sandstones found around the Mississippi embayment (Potter-McIntyre et al., 2018). Both Clayton sand samples yield bimodal age distributions, with one mode of Grenville age (900-1300 Ma) and another mode of Acadian/Taconic age (320-490 Ma), whereas one sample (ML-19-5) shows a minor mode from 500-560 Ma, reflecting a Pan-African signal. These results support conclusions of Blum and Pecha (2014) and Potter-McIntyre et al. (2018) that indicate Appalachian input both from the northeast and possibly from the mid-continent. However, given the presence of impact signatures found at Moscow Landing in previous studies (Smit et al., 1996; Savrda, 2018), we cannot rule out that rare Pan-African zircon grains were delivered as ejecta derived from the target rocks of the Chicxulub impact on the Yucatan peninsula. More work is needed to distinguish between zircons derived from the Yucatan, Illinois basin, and Carolina terrane to fully understand the provenance of the Clayton sands at Moscow Landing. Coupling detrital zircon ages with Th/U values as described by Jackson et al. (2021) could provide a way to further distinguish between metamorphic and igneous sources. Looking at the morphology (euhedral vs rounded) of the zircon grains can provide information about transport distance and relative age.

The current study of detrital zircons provides no concrete solution to the mystery of whether the Clayton sand bodies were created as incised valley fills or from Chicxulub impact-induced megawaves. However, the data presented herein reinforces previous studies examining Gulf coast paleodrainage, provides additional important information about the Moscow Landing section, and, in documenting the first *potential* Chicxulub impact-related zircons in Alabama, lay the groundwork for future studies of other K-Pg sections elsewhere in the state.

REFERENCES

- Alvarez, L.W., Alvarez W., Asaro, F., 1980, Michel, H.V., Extraterrestrial Cause for the Cretaceous-Tertiary Extinction: *Science*, v. 208, pp. 1095-1108
- Blum, M., Pecha, M., 2014, Mid-Cretaceous to Paleocene North American drainage reorganization from detrital zircons: *Geology*, v. 42, no. 7, pp. 607-610
- Cavosie, A.J., Biren, M.B., Hodges, K.V., Warthro, J., Horton Jr, J.W., Koeberl, C., 2020, Dendritic reidite from the Chesapeake Bay impact horizon, Ocean Drilling Program Site 1073 (offshore northeastern USA): A fingerprint of distal ejecta? *Geology*, v. 49, no. 2, pp. 201-205
- Chen, G., Robertson, A. H. F., 2020, User's guide to the interpretation of sandstones using whole-rock chemical data, exemplified by sandstones from Triassic to Miocene passive and active margin settings from the Southern Neotethys in Cyprus: *Sedimentary Geology*, v. 400, pp. 1-22
- Dennis, A.J., Wright, J.E., 1997, The Carolina terrane in northwestern South Carolina, USA: Late Precambrian-Cambrian deformation and metamorphism in a peri-Gondwanan oceanic arc: *Tectonics*, v. 16, no. 3, pp. 460-473
- Gifford, J.N., Vitale, E.J., Platt, B.F., Malone, D.H., Widanagamage, I.H., 2020, Detrital Zircon Provenance and Lithofacies Associations of Montmorillonitic Sands in the Maastrichtian Ripley Formation: Implications for Mississippi Embayment Paleodrainage Patterns and Paleogeography: *Geosciences*, v. 10, no. 80
- Gulick, S.P.S., Bralower, T.J., Ormo, J., Hall, B., Grice, K., Schaefer, B., Lyons, S., Freeman, K.H., Morgan, J.V., Artemieva, N., Kaskes, P., de Graff, S.J., Whalen, M.T., Collins, G.S., Tikoo, S.M., Verhagen, C., Christeson, G.L., Claeys, P., Collen, M.J.L., Goderis, S., Goto, K., Grieve, R.A.F., McCall, N., Osinski, G.R., Rae, A.S.P., Riller, U., Smit, J., Vajda, V., Wittmann, A., Expedition 364 Scientists, 2019, The first day of the Cenozoic: *PNAS*, v. 116, pp. 19342-19351
- Hart, M.B., FitzPatrick, M.E.J., Smart, C.W., 2016, The Cretaceous/Paleogene boundary: Foraminifera, sea grass, sea level change and sequence stratigraphy: *Palaeogeography, Palaeoclimatology, Palaeoecology*, v. 44, pp. 420-429
- Herron, M.M., 1988, Geochemical Classification of Terrigenous Sands and Shales from Core or Log Data: *Journal of Sedimentary Petrology*, v. 58, no. 5, pp. 820-829

- Hiess, J., D. J. Condon, N. McLean, and S. R. Noble, 2012, $^{238}\text{U}/^{235}\text{U}$ Systematics in Terrestrial Uranium-Bearing Minerals. *Science*, v. 335 (6076), pp. 1610–1614.
- Hildebrand, A.R., Penfield, G.T., Kring, D.A., Pilkington, M., Camargo Z, A., Jacobsen, S.B., Boynton, W.V., 1991, Chicxulub Crater: A possible Cretaceous/Tertiary boundary impact crater on the Yucatan Peninsula, Mexico: *Geology*, v. 19, pp. 867-871
- Horstwood, M. S. A., G. L. Foster, R. R. Parrish, S. R. Noble, and G. M. Nowell, 2003, Common-Pb corrected *in situ* U–Pb accessory mineral geochronology by LA-MC-ICP-MS. *Journal of Analytical Atomic Spectrometry*, v. 18 (8), pp. 837–846
- Ingle, S., Mueller, P.A., Heatherington, A.L., Kozuch, M., 2003, Isotopic evidence for the magmatic and tectonic histories of the Carolina terrane: implications for stratigraphy and terrane affiliation: *Tectonophysics*, v. 371, pp. 187-211
- Jackson Jr, W.T., McKay, M.P., Beebe, D.A., Mullins, C., Ionescu, A., Shaulis, B., Barbeau Jr, D.L., 2021, Late Cretaceous Sediment Provenance of the Eastern Gulf Coastal Plain (U.S.A.) Based on Detrital-Zircon U-Pb ages and Th/U Values: *Journal of Sedimentary Research*, v. 91, pp. 1025-1039
- Johnson, D.M., Hooper, P.R, Conrey, R.M., 1999, XRF Analysis of rocks and Minerals for Major and Trace Elements on a Single Low dilution Li-tetraborate Fused Bead, *Advances in X-Ray Analysis*, v. 41, pp. 843-867
- Kamo, S.L., Krogh, T.E., 1995, Chicxulub crater source for shocked zircons crystals from the Cretaceous-Tertiary boundary layer, Saskatchewan: Evidence from new U-Pb data: *Geology*, v. 23, no. 3, pp. 281-284
- Kamo, S.L., Lana, C., Morgan, J.V., 2011, U-Pb ages of shocked zircons grains link distal K-Pg boundary sites in Spain and Italy with the Chicxulub impact: *Earth and Planetary Science Letters*, v. 310, pp. 401-408
- Kettrup, B., Deutsch, A., 2003, Geochemical variability of the Yucatan basement: Constraints from crystalline clasts in Chicxulub impactites: *Meteoritics and Planetary Science*, v. 38, no. 7, pp. 1079-1092
- Klepeis, K. A., M. L. Crawford, and G. Gehrels, 1998, Structural history of the crustal-scale Coast shear zone north of Portland Canal, southeast Alaska and British Columbia. *Journal of Structural Geology*, v. 20 (7), pp. 883–904
- Kring, D.A., Claeys, P., Gulick, S.P.S., Morgan, J.V., Collins, G.S., 2017, Chicxulub and the Exploration of Large Peak-Ring Impact Craters through Scientific Drilling: *GSA Today*, v. 27
- Krogh T.E., Kamo, S.L., Sharpton, V.L., Marin, L.E., Hildebrand, A.R., 1993b, U-Pb ages of single shocked zircons linking distal K/T ejecta to the Chicxulub crater: *Nature*, v. 366, pp. 731-734

- Krogh, T.E., Kamo, S.L., Bohor, B.F., 1993a, Fingerprinting the K/T impact site and determining the time of impact by U-Pb dating of single shocked zircons from distal ejecta: *Earth and Planetary Science Letters*, v. 119, pp. 425-429
- Larina, E., Garb, M., Landman, N., Dastas, N., Thibault, N., Edwards, L., Phillips, G., Rovelli, R., Myers, C., Naujokaiyte, J., 2016, Upper Maastrichtian ammonite biostratigraphy of the gulf Coastal Plain (Mississippi Embayment, southern USA): *Cretaceous Research*, v. 60, pp. 128-151
- Lawton, T.F., Shipley, K.W., Aschoff, J.L., Giles, K.A., Vega, F.J., 2004, Basinward transport of Chicxulub ejecta by tsunami-induced backflow, La Popa basin, northeastern Mexico, and its implications for distribution of impact-related deposits flanking the Gulf of Mexico: *Geology*, v. 33, no. 2, pp. 81-84
- Mancini, E.A., Tew, B.H., Smith, C.C., 1989, Cretaceous-Tertiary Contact. Mississippi and Alabama: *Journal of Foraminiferal Research*, v. 19, pp. 93-104
- Mattinson, J. M., 2010, Analysis of the relative decay constants of ^{235}U and ^{238}U by multi-step CA-TIMS measurements of closed-system natural zircon samples. *Chemical Geology*, v. 275, pp. 186-198
- Paces J. B. and J. D. Miller Jr., 1993, Precise U-Pb ages of Duluth Complex and related mafic intrusions, northeastern Minnesota: Geo-chronological insights to physical, petrogenetic, paleomagnetic, and tectonomagmatic processes associated with the 1.1 Ga Midcontinent Rift System. *J. Geophys. Res.*, v. 98, pp. 13997–14013
- Paton, C., J. D. Woodhead, J. C. Hellstrom, J. M. Herget, A. Greig, and R. Maas, 2010, Improved laser ablation U-Pb zircon geochronology through robust downhole fractionation correction. *Geochemistry, Geophysics, Geosystems*, v. 11 (3)
- Paton, C., J. Hellstrom, B. Paul, J. Woodhead, and J. M. Herget, 2011, Iolite: Freeware for the visualisation and processing of mass spectrometric data. *Journal of Analytical Atomic Spectrometry*, v. 26 (12), pp. 2508
- Petrus, J. A. and B. S. Kamber, 2012, VizualAge: A Novel Approach to Laser Ablation ICP-MS U-Pb Geochronology Data Reduction. *Geostandards and Geoanalytical Research*, v. 36 (3), pp. 247–270
- Pitakpaivan, K., Byerly, G.R., Hazel, J.E., 1994, Pseudomorphs of impact spherules from a Cretaceous-Tertiary boundary section at Shell Creek, Alabama: *Earth and Planetary Science Letters*, v. 124, pp. 49-56
- Potter-McIntyre, S.L., Breeden, J.R., Malone, D.H., 2018, A Maastrichtian birth of the Ancestral Mississippi River system: Evidence from the U-Pb detrital geochronology of the McNairy Sandstone, Illinois, USA: *Cretaceous Research*, v. 91, pp. 71-79

Ross, C.H., Stockli, D.F., Rasmussen, C., Gulick, S.P.S., de Graaff, S.J., Claeys, P., Zhao, J., Xiao, L., Pickersgill, A.E., Schmieder, M., Kring, D.A., Wittmann, A., Morgan, J.V., IODP 364 Science Party, 2019, Zircons U-Pb geochronology and trace elements of the Chicxulub impact structure basement, LPI contributions no. 2136, 50th Annual Lunar and Planetary Science Conference

Savrda, C.E., 1993, Ichnosedimentologic evidence for a noncatastrophic origin of Cretaceous-Tertiary boundary sands in Alabama: Geology, v. 21, pp. 1075-1078

Savrda, C.E., 2018, Revisiting the origins of Clayton sand bodies at the K-Pg transition, Moscow Landing, Western Alabama: Stratigraphic relations, sedimentology, and ichnology: PALAIOS, v. 33, pp. 555-567

Schmieder, M., Shaults, B.J., Lapen, T.J., Kring, D.A., 2017, U-Th-Pb systematics in zircon and apatite from the Chicxulub impact crater, Yucatan, Mexico, Geology Magazine, v. 155, no. 6, pp. 1330-1350

Schmitz, M.D., S. A. Bowring, T. R. Ireland, 2003, Evaluation of Duluth Complex anorthositic series (AS3) zircon as a U–Pb geochronological standard: new high- precision isotope dilution thermal ionization mass spectrometry results. Geochimica et Cosmochimica Acta, v. 67, pp. 3665–3672

Sharpton, V.L., Burke, K.V., Carmago-Zanoguera, A., Hall, S.A., Lee, D.S., Marin, L.E., Suarez-Reynoso, G., Quezada-Muneton, J.M., Spudis,P.D., Urrutia-Fucugauchi, J., 1993, Chicxulub Multiring Impact Basin: Size and Other Characteristics Derived from Gravity Analysis: Science, v. 261, pp. 1594-1567

Slama, J., J. Kosler, D. J. Condon, J. L. Crowley, A. Gerdes, J. H. Hanchar, M. S. A. Horstwood, G. A. Morris, L. Nasdala, N. Norberg, U. Schaltegger, B. Schoene, M. N. Tubrett, and M. J. Whitehouse, 2008, Plesovice zircon – A new natural reference material for U-Pb and Hf isotopic microanalysis. Chemical Geology, v 249, pp. 1-35

Smit, J., Roep, Th.B., Alvarez, W., Montanari, A., Claeys, P., Grajales-Nishimura, J.M., Bermudez, J., 1996, Course-grained, clastic complex at the K-T boundary around the Gulf of Mexico: Deposition by the tsunami waves induced by the Chicxulub impact *in* special paper 307: Geological Society of America, pp. 151-182

Smit, J., Roep, Th.B., Alvarez, W., Montanari, S., Claeys, P., 1994, Stratigraphy and Sedimentology of KT Clastic Beds in the Moscow Landing (Alabama) Outcrop: Evidence for Impact-Related Earthquakes and Tsunami: LPI Contributions no. 825, pp. 119-120

Thomas, W.A., Gehrels, G.E., Greb, S.F., Nadon, G.C., Satkoski, A.M., Romero, M.C., 2017, Detrital zircons and sediment dispersal in the Appalachian foreland: Geosphere, v. 13, no. 6, pp. 2206-2230

- Thomas, W.A., Gehrels, G.E., Sundell, K.E., Greb, S.T., Finzel, E.S., Clark, R.J., Malone, D.H., Hampton, B.A., Romero, M.C., 2020, Detrital zircons and sediment dispersal in the Eastern Midcontinent of North America: *Geosphere*, v. 16, no. 3, pp. 817-843
- Ver Hoeve, T. J., J. S. Scoates, C. J. Wall, D. Weis, and M. Amini, 2018, Evaluating downhole fractionation corrections in LA-ICP-MS U-Pb zircon geochronology. *Chemical Geology*, v. 483, pp. 201–217
- Vermeesch, P., 2012, On the visualization of detrital age distributions: *Chemical Geology*, v. 312-313, pp. 190-194
- Vermeesch, P., 2018, IsoplotR: A free and open toolbox for geochronology. *Geoscience Frontiers*, v. 9, pp. 1479-1493
- Wortmean, G.L., Samson, S.D., Hibbard, J.P., 2000, Precise U-Pb Zircon Constraints on the Earliest Magmatic History of the Carolina Terrane: *Journal of Geology*, v. 108 pp.321-338
- Zhang, M., Salje, E.K.H., Capitan, G.C., Leroux, H., Clark, A.M., Schluter, J., Ewing, R.C., 2000, Annealing of α -decay damage in zircon: a Raman spectroscopic study: *Journal of Physics: Condensed Matter*, v. 12, pp. 3131-3148